Supporting Information

Iacob *et al.* 10.1073/pnas.0811912106

SI Materials and Methods

Materials. 96% formic acid, deuterium oxide (99.9%), dithiotreitol, sodium chloride and pepsin were purchased from Sigma-Aldrich. Acetonitrile and water (W5–4 HPLC grade) were purchased from Fisher Scientific. Potassium phosphate was purchased from EMD Biosciences. All chemicals were used without further purification unless otherwise specified.

Z′Lyte Kinase Assay. Briefly, recombinant Abl proteins were incubated with ATP (50 μM) and Tyr-2 substrate (2 μM) in a final volume of 10 μL and the reaction was incubated for 45 min at room temperature. Development reagent, containing a protease that digests the nonphosphorylated substrate peptide, was then added and the reaction incubated for another 60 min before addition of the proprietary stop reagent. Fluorescence was assessed at an excitation wavelength of 400 nm; coumarin fluorescence and the fluorescein FRET signal were monitored at 445 nm and 520 nm, respectively. Reactions containing unphosphorylated peptide and kinase without ATP served as the 0% phosphorylation control, whereas a stoichiometrically phosphorylated peptide was used as a 100% phosphorylation control. Reaction endpoints were calculated as emission ratios of coumarin fluorescence divided by the fluorescein FRET signal, and normalized to the ratio obtained with the 100% phosphorylation control. Each condition was assayed in quadruplicate, and each experiment was performed at least 3 times. Results are presented as the mean % phosphorylation $\pm$ SD.

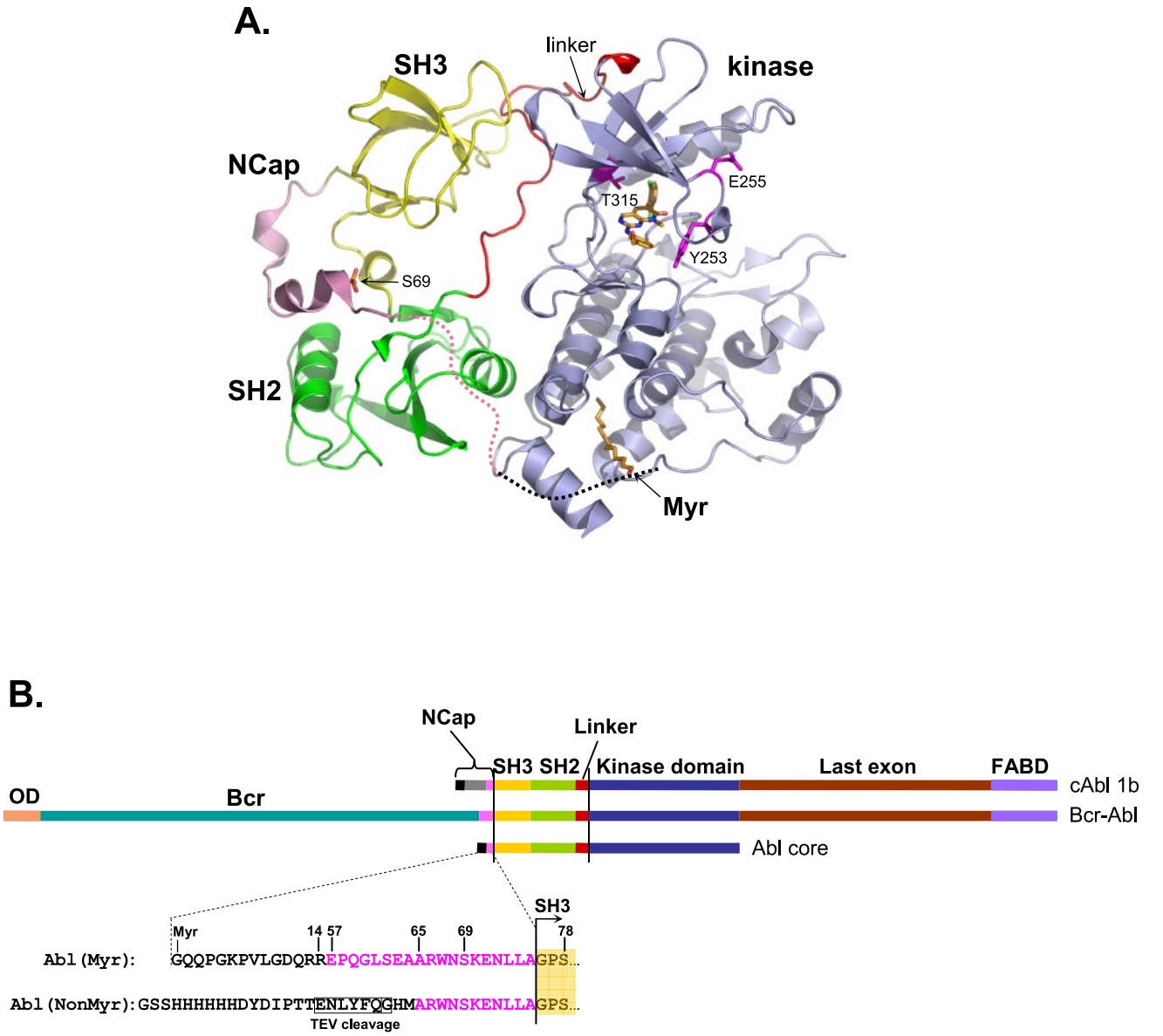

Fig. S1. The crystal structure of c-Abl (*A*), PDB entry 2FO0 (1), and the domains of Abl and Bcr-Abl (*B*), drawn to scale. c-Abl consists of an N-terminal region known as the Cap (NCap), SH3 and SH2 domains, a linker sequence, and the kinase domain, followed by a large C-terminal domain (the last exon region or C-terminal domain) important for subcellular localization and protein/DNA binding (2, 3). Fusion of Bcr to Abl removes the first 46 aa of the NCap producing a protein (Bcr-Abl) almost twice the size of c-Abl. The tyrosine kinase core of c-Abl (referred to as Abl core), consists of the NCap, SH3, and SH2; the linker and the kinase domain remains mostly intact in Bcr-Abl. The constructs used in this study were the Abl core protein expressed in either Sf9 cells where Abl core became myristoylated, denoted as Abl(Myr), or the Abl core protein expressed in bacteria where it was not myristoylated, denoted as Abl(NonMyr), see Fig. S2 below. Abl(Myr) is identical to the protein used to obtain the crystal structure shown in *A*, PDB entry code 2FO0 (1). The color coding is consistent between panel A and panel B. All numbering is according to the sequence for Abl 1b except for the numbers used to indicate the mutations T315, E255, and Y253, which are labeled according to the established convention.

1. Nagar B, *et al.* (2006) Organization of the SH3-SH2 unit in active and inactive forms of the c-Abl tyrosine kinase. *Mol Cell* 21:787–798.
2. Pendergast AM (2002) The Abl family kinases: Mechanisms of regulation and signaling. *Adv Cancer Res* 85:51–100.
3. Hantschel O, Superti-Furga G (2004) Regulation of the c-Abl and Bcr-Abl tyrosine kinases. *Nat Rev* Mol Cell Biol 5:33–44.

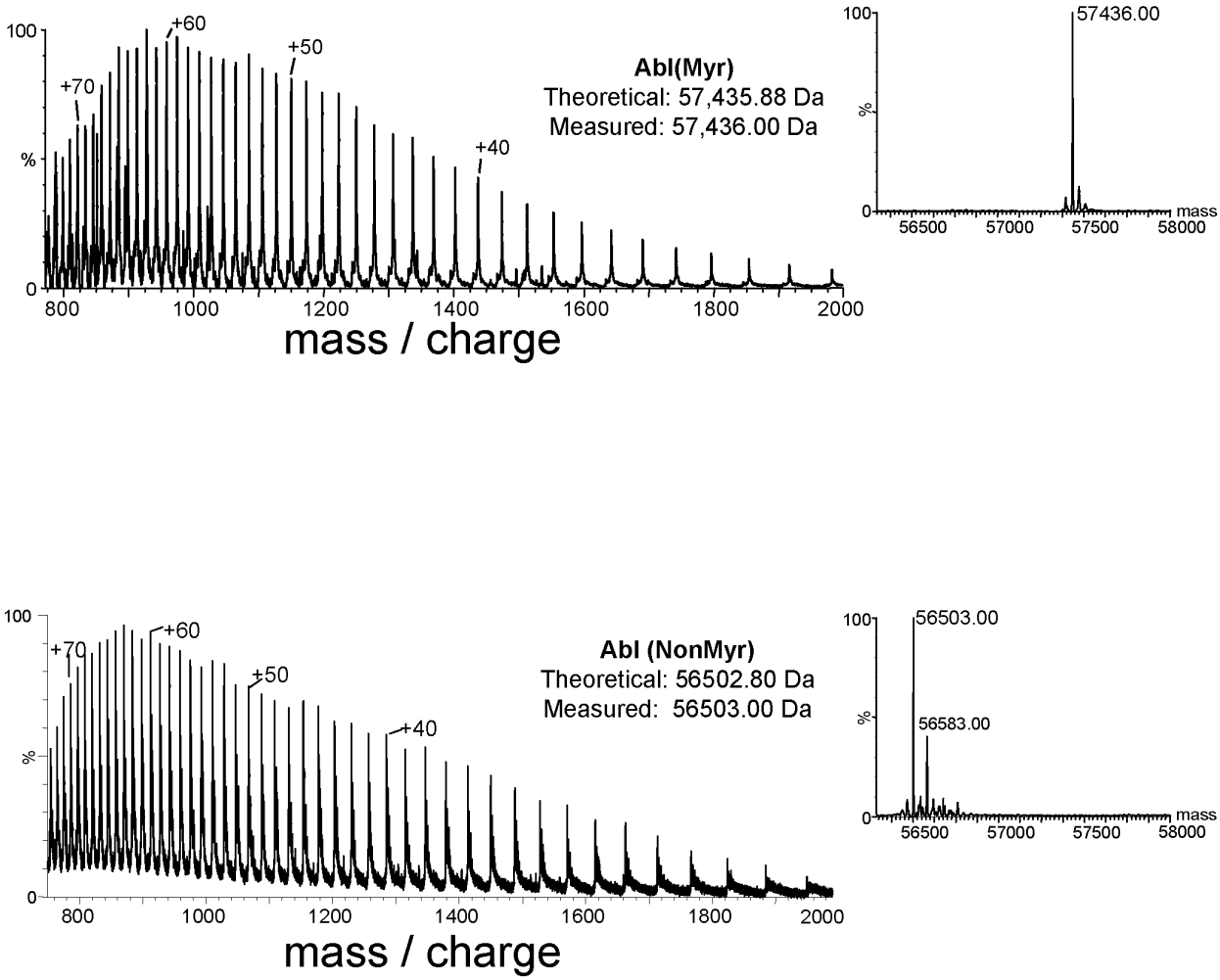

Fig. S2. Mass spectra of the Abl proteins. The raw *m/z* data are shown on the *Left* and the transformed, mass only spectra shown on the *Right*. The measured and theoretical molecular masses are indicated. Wild-type Abl core, T315I, E255V and Y253H mutants were overexpressed in Sf9 insect cells coexpressing YopH, as described for wild-type Abl (1). To prepare Abl core in bacteria, referred to as Abl(NonMyr), the procedure described in ref. 2 was followed. A pET-28a vector bearing Abl residues 65–534 (Abl 1b numbering) was coexpressed with YopH phosphatase in *E. coli* BL21DE3 cells. Cultures were grown to an OD_{600} of 1.2 at 37 °C, cooled for 1 h with shaking at 18 °C before induction for 16 h at 18 °C with 0.2 mM IPTG. Cells were harvested by 10 min of centrifugation at 7,000 $\times$ *g* at 4 °C and resuspended in 50 mM Tris·HCl, pH 8.0, 500 mM NaCl, 5% glycerol, 25 mM imidazole (buffer A). Lysates were clarified by centrifugation at 40,000g at 4 °C for 40 min. The supernatant was loaded onto a Ni affinity column (HisTrap FF; GE Lifescience), equilibrated with buffer A. The column was washed with 5 column volumes of buffer A, and Abl protein was eluted with a linear gradient of 0–50% of buffer B (Buffer A plus 0.5 M imidazole). Fractions containing the kinase were pooled and dialyzed against 20 volumes of 20 mM Tris (pH 8.0), 100 mM NaCl, 5% glycerol, 1 mM DTT with a 13-kDa molecular mass cutoff membrane. Subsequent anion exchange chromatography (HiTrap Q FF; GE Lifescience) was used to remove protease and phosphatase contaminants. Proteins were eluted with a linear gradient of 0–35% elution buffer (20 mM Tris, pH 8.0, 5% glycerol, 1 mM DTT plus 1 M NaCl). For intact protein mass spectral analysis, the proteins were injected onto a POROS 20 R2 protein trap and desalted with 0.05% trifluroacetic acid (TFA) at a flow rate of 100 μL/min. The proteins were eluted into the mass spectrometer, using a linear 15–75% (vol/vol) acetonitrile gradient over 4 min at 50 μL/min, using a Shimadzu HPLC system (LC-10ADvp). Intact protein analyses were performed on an LCT-Premier instrument (Waters) equipped with a standard electrospray source. The capillary voltage was 3.2 kV and the cone voltage of 35 V. Nitrogen was used as desolvation gas. A source temperature of 175 °C and a desolvation temperature of 80 °C were applied. The instrument was calibrated by infusing a solution of 500 fmol/μL myoglobin and the mass accuracy was $<$10 ppm.

1. Chen S, Brier S, Smithgall TE, Engen JR (2007) The Abl SH2-kinase linker naturally adopts a conformation competent for SH3 domain binding. *Protein Sci* 16:572–581.
2. Seeliger MA, *et al.* (2005) High yield bacterial expression of active c-Abl and c-Src tyrosine kinases. *Protein Sci* 14:3135–3139.

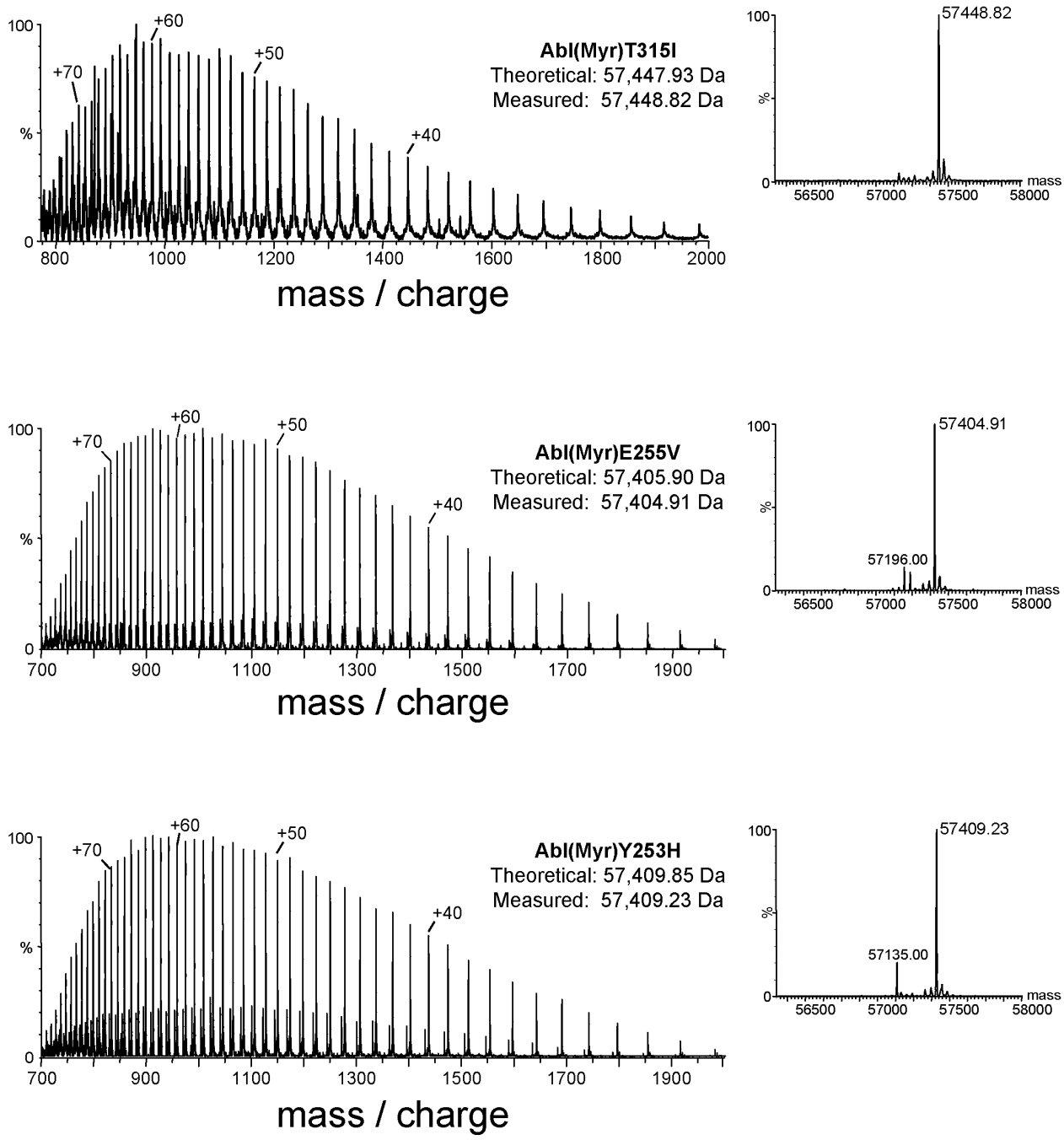

Fig. S2 (continued).

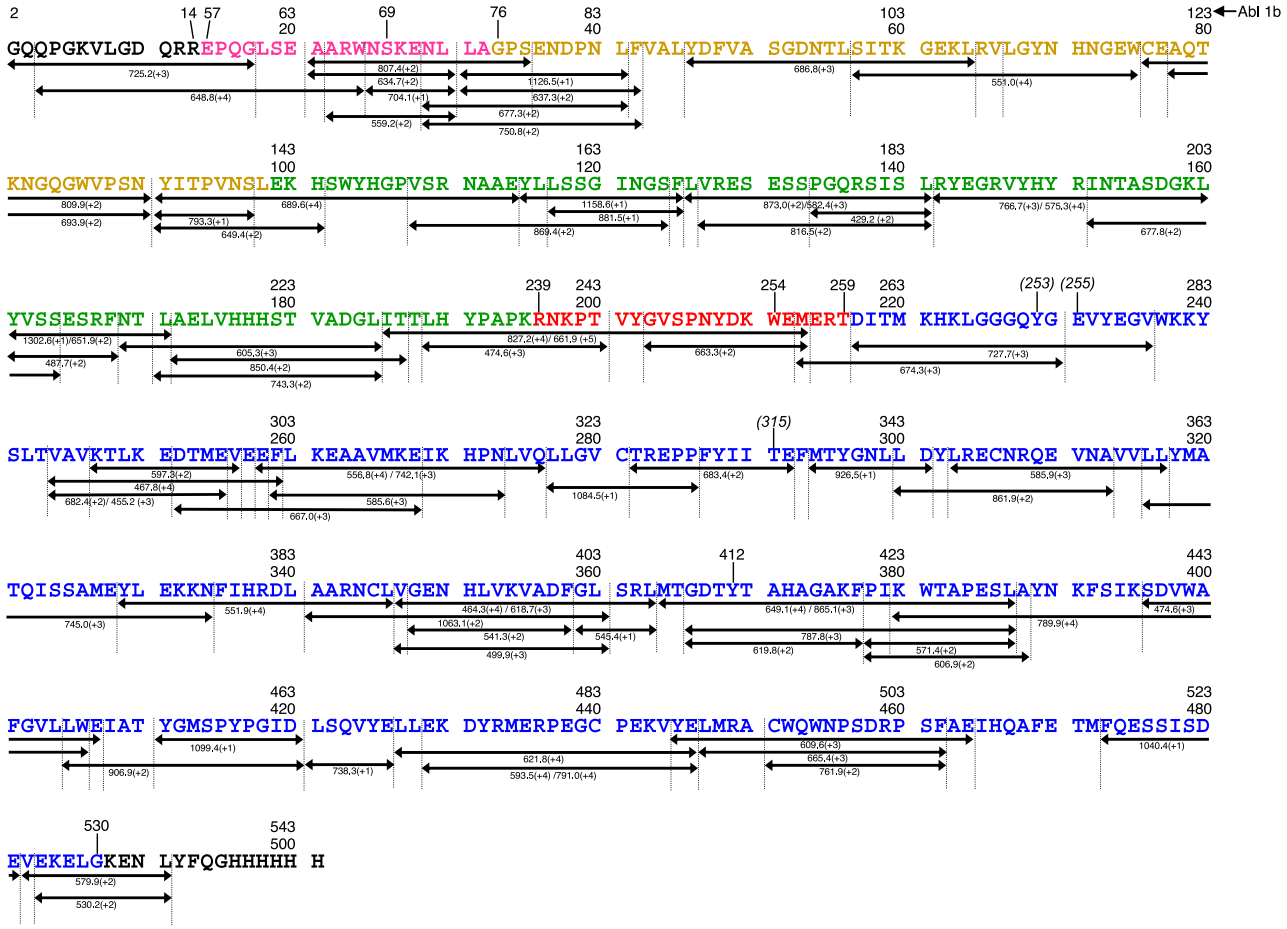

Fig. S3. Peptic peptide map of Abl(Myr). Each arrow under the sequence indicates a peptic peptide, along with the *m/z* and charge state. The sequence coloring corresponds to the domain designation as described in ref. 1. There are deletions in the NCap in this Abl(Myr), as described in ref. 1. The protein sequence is numbered for the Abl 1b sequence (top numbers) and the Abl(Myr) protein itself (bottom numbers). For the peptide designation throughout the main text, we have used the top numbers (Abl 1b). The location of the mutations 253, 255, and 315 are indicated, although this numbering corresponds to the established convention of using Abl 1a sequence for numbering (2). To convert from Abl 1b to Abl 1a sequence numbering, subtract 19 from the Abl 1b number. Identification of the peptic fragments was accomplished through a combination of exact mass analysis and MS^E (3), using custom Identity Software from Waters. MS^E was performed by a series of low-high collision energies ramping from 5 to 25 V, therefore ensuring proper fragmentation of all of the peptic peptides eluting from the LC system.

1. Nagar B, *et al.* (2006) Organization of the SH3-SH2 unit in active and inactive forms of the c-Abl tyrosine kinase. *Mol Cell* 21:787–798.
2. Gorre ME, *et al.* (2001) Clinical resistance to STI-571 cancer therapy caused by BCR-ABL gene mutation or amplification. *Science* 293:876–880.
3. Plumb RS, *et al.* (2006) UPLC/MS(E): A new approach for generating molecular fragment information for biomarker structure elucidation. *Rapid Commun Mass Spectrom* 20:1989–1994.

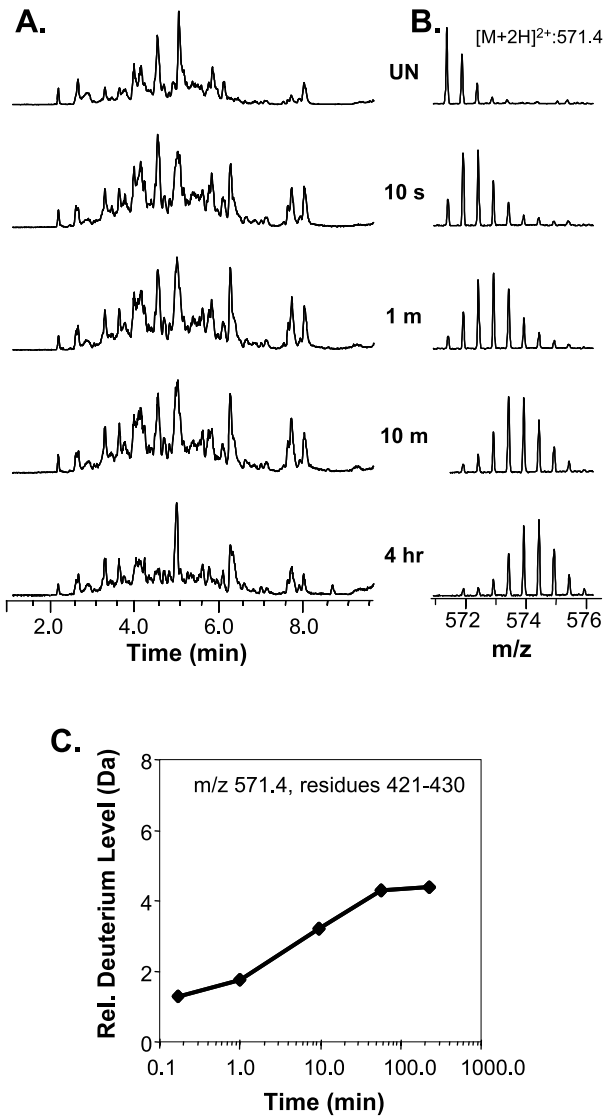

Fig. S4. Example HX MS data for Abl(Myr). (*A*) Chromatograms of the UPLC separation at 0 °C of peptic digests of Abl(Myr) after incubation in deuterium for the amounts of time indicated. UN, undeuterated. To obtain these data, deuteration was performed as described in the Methods section. Each frozen sample was thawed rapidly to 0 °C and incubated with pepsin at a ratio of 1:1 (weight:weight) for 5 min at 0 °C. The resulting peptides were injected into a custom Waters nanoACQUITY UPLC system and analyzed as described in ref. 1. The cooling chamber of the UPLC system, which housed all of the chromatographic elements was held at 1 °C for the entire time of the measurements. The injected peptides were trapped and desalted for 3 min at 100 μL/min and then separated in 6 min by an 8–40% acetonitrile:water gradient at 40 μL/min. The separation column was a 1.0 $\times$ 100.0 mm ACQUITY UPLC C18 BEH (Waters) containing 1.7 μm particles and the back pressure averaged 8800 psi at 1 °C. The UPLC step was performed with protiated solvents, thereby removing deuterium from side chains and amino/carboxyl terminus that exchange much faster than amide linkages (2). (*B*) Example electrospray MS data illustrating the quality of the mass spectra obtained for >90% of the peptic peptides of Abl. These data are for the peptic peptide corresponding to *m/z* 571.4, +2 charge state, sequence ^{421}PIKWTAPESL^{430}. Residues 421–430 represent the short alpha helical region just after the activation loop in the kinase domain. Peptide numbering is according to the Abl 1b sequence; see *SI Text*, Fig. S3 for details. The mass spectra were obtained with a Waters QTOF Premier equipped with standard ESI source. Mass spectra were acquired over an *m/z* range of 100 to 2,000. Mass accuracy was ensured by calibration with 100 fmol/μL GFP, and was <10 ppm throughout all experiments. A totally deuterated Abl control could not be reliably prepared. The average amount of back-exchange using this UPLC and ESIMS experimental setup was 18–25%, based on analysis of highly deuterated peptide standards. There was no correction made for back-exchange and all results are reported as relative deuterium level (3). (*C*) Deuterium uptake for the peptide data shown in panel B. Mass spectra were processed with the software HX-Express (4) where the deuteration levels were calculated by subtracting the centroid of the isotopic distribution for peptide ions of undeuterated protein from the centroid of the isotopic distribution for peptide ions from the deuterium labeled sample. The *y* axis maximum corresponds to the theoretical maximum amount of deuterium that could be incorporated into this peptide. The deuterium uptake curve indicates that this region of Abl(Myr) incorporated ≈1 deuterium at early time points and ≈5 deuterium atoms at later time points. This peptide could incorporate a maximum of 8 deuterium atoms; therefore it can be concluded that this region is significantly structured and resistant to exchange at early times but is mobile in solution allowing eventual deuteration of a large percentage of the available amide hydrogens.

1. Wales TE, Fadgen KE, Gerhardt GC, Engen JR (2008) High-speed and high-resolution UPLC separation at zero degrees celsius. *Anal Chem* 80:6815–6820.
2. Englander SW, Kallenbach NR (1983) Hydrogen exchange and structural dynamics of proteins and nucleic acids. *Q Rev Biophys* 16:521–655.
3. Wales TE, Engen JR (2006) Hydrogen exchange mass spectrometry for the analysis of protein dynamics. *Mass Spectrom Rev* 25:158–170.
4. Weis DD, Engen JR, Kass IJ (2006) Semi-Automated Data Processing of Hydrogen Exchange Mass Spectra Using HX-Express. *J Am Soc Mass Spectrom* 17:1700–1703.

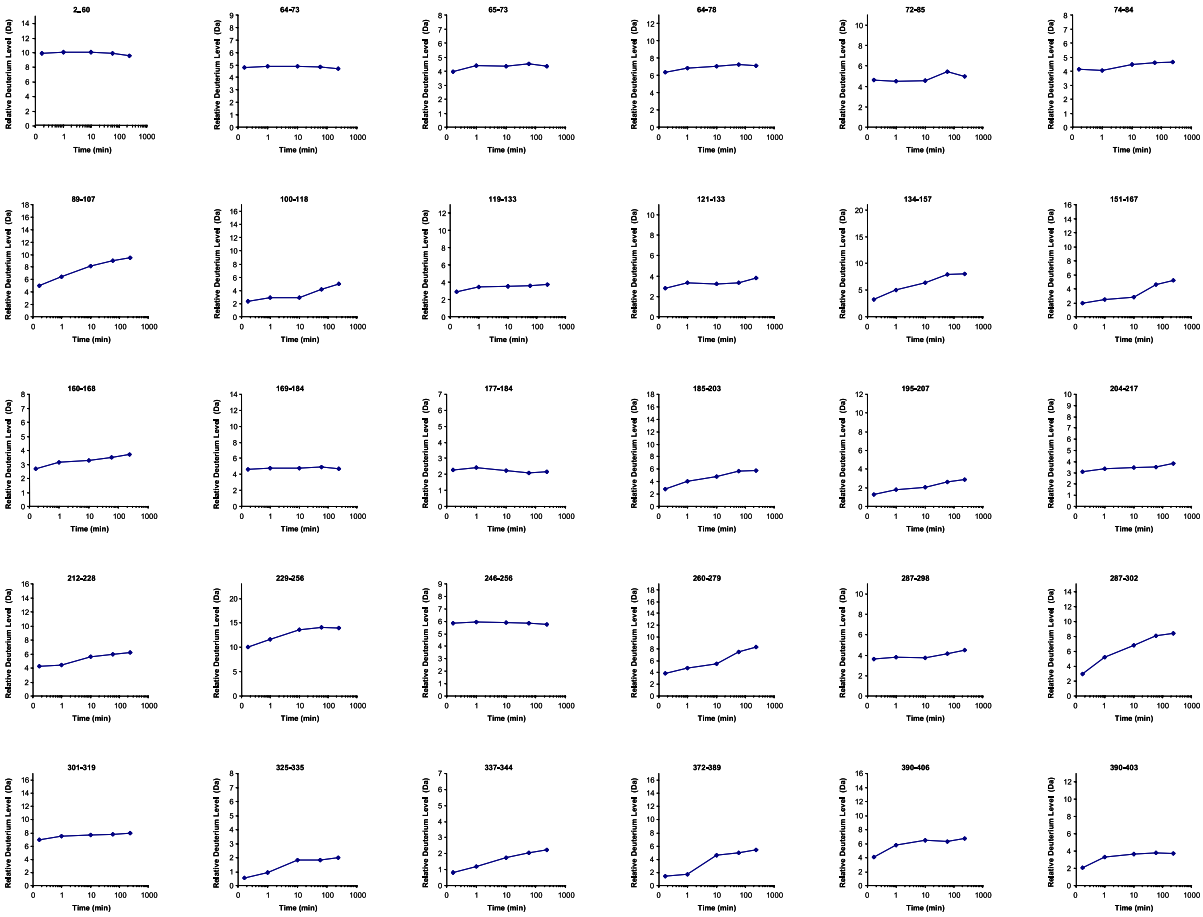

Fig. S5. Relative deuterium incorporation curves for Abl(Myr) pepsin fragments identified in SI, Fig. S3. The maximum of the *y* axis in each graph is the maximum amount of deuterium that could be incorporated. The data were obtained and processed as described in Fig. S4. No corrections have been made for back-exchange thus the absolute value of each deuterium level is ≈18–25% higher than plotted based on totally deuterated standards [described in detail in Wales TE, Engen JR (2006) *Mass Spectrom Rev* 25:158–170]. Although the entire experiment was performed in duplicate, only 1 dataset is shown. The error of determining the deuterium levels was ±0.20 Da in the experimental setup used so in most cases, the error bars for each point are approximately the size of the point.

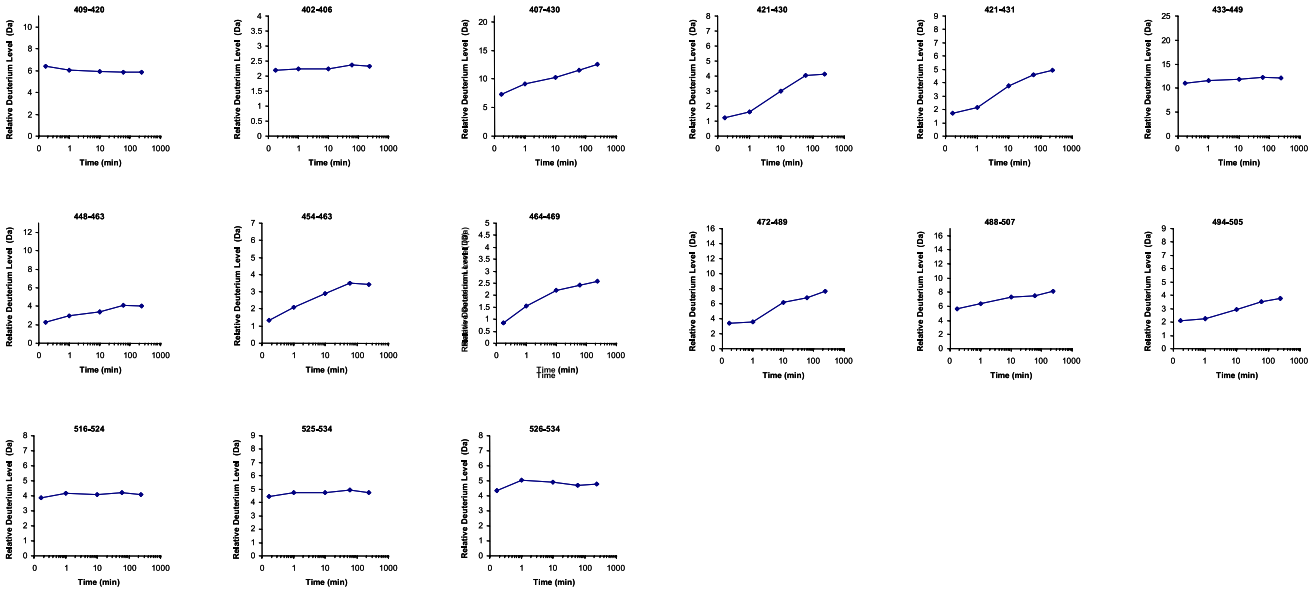

Fig. S5 (continued).

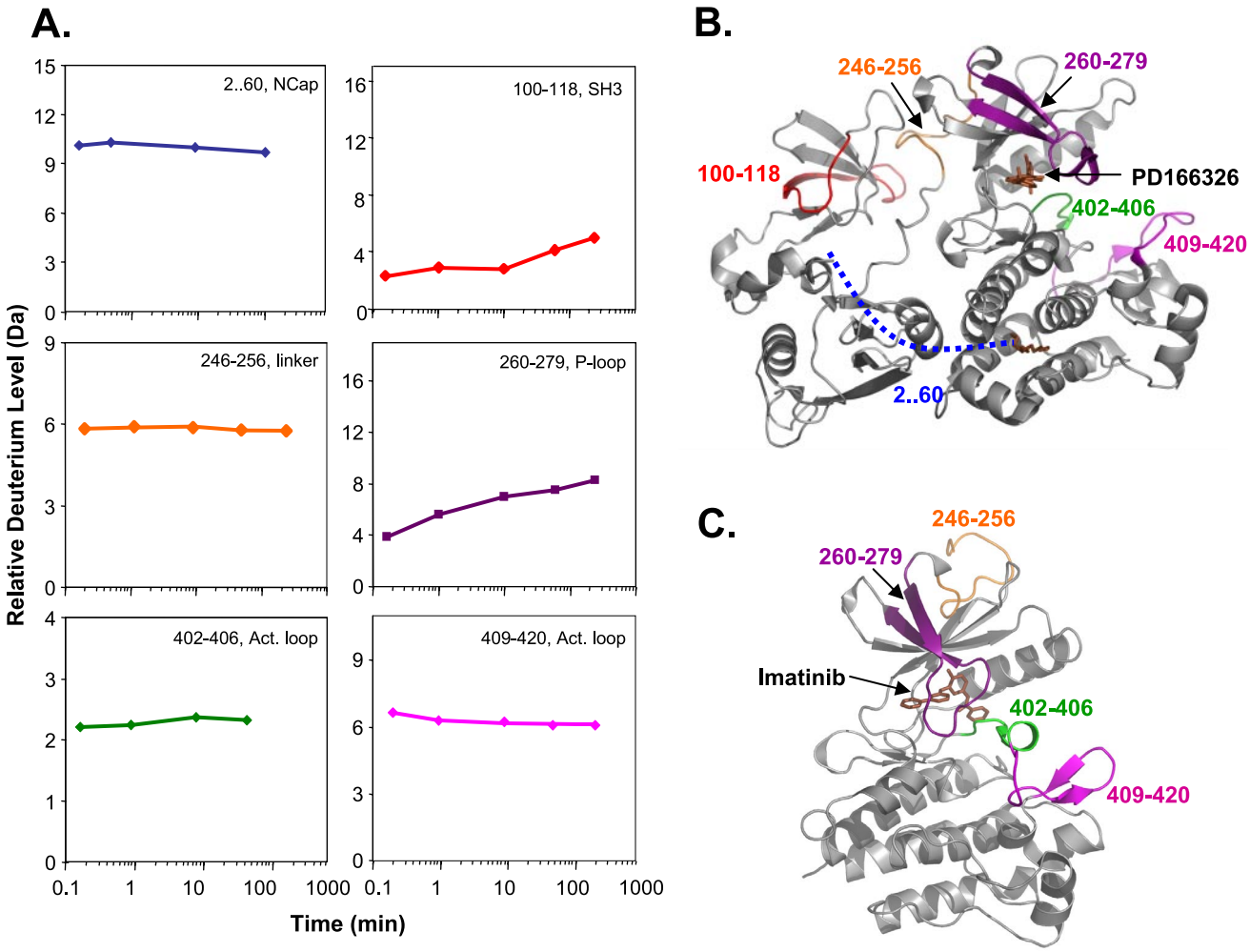

Fig. S6. Deuterium incorporation into selected regions of Abl(Myr). (*A*) Data are shown for 6 representative peptides from functionally interesting and important parts of Abl. Data for peptides can be found in the SI, Fig. S5. Note that 2.60 designates the peptide covering the 17 residues within the Abl(Myr) sequence numbered 2–60, bearing in mind that there are deletions in this area (see Fig. S1) and that all residues 2 through 60 are not present. (*B* and *C*) Location of the peptides in *A*, shown on crystal structure PDB entry 2FO0, cocrystallized with PD166326 (1) or on the crystal structure of the kinase domain only PDB entry 1FPU, cocrystallized with imatinib (2). The HX MS data are more consistent with the structure in panel B, where the peptides near the activation loop are more solvent exposed and less protected.

1. Nagar B, *et al.* (2006) Organization of the SH3-SH2 unit in active and inactive forms of the c-Abl tyrosine kinase. *Mol Cell* 21:787–798.
2. Schindler T, *et al.* (2000) Structural mechanism for STI-571 inhibition of abelson tyrosine kinase. *Science* 289:1938–1942.

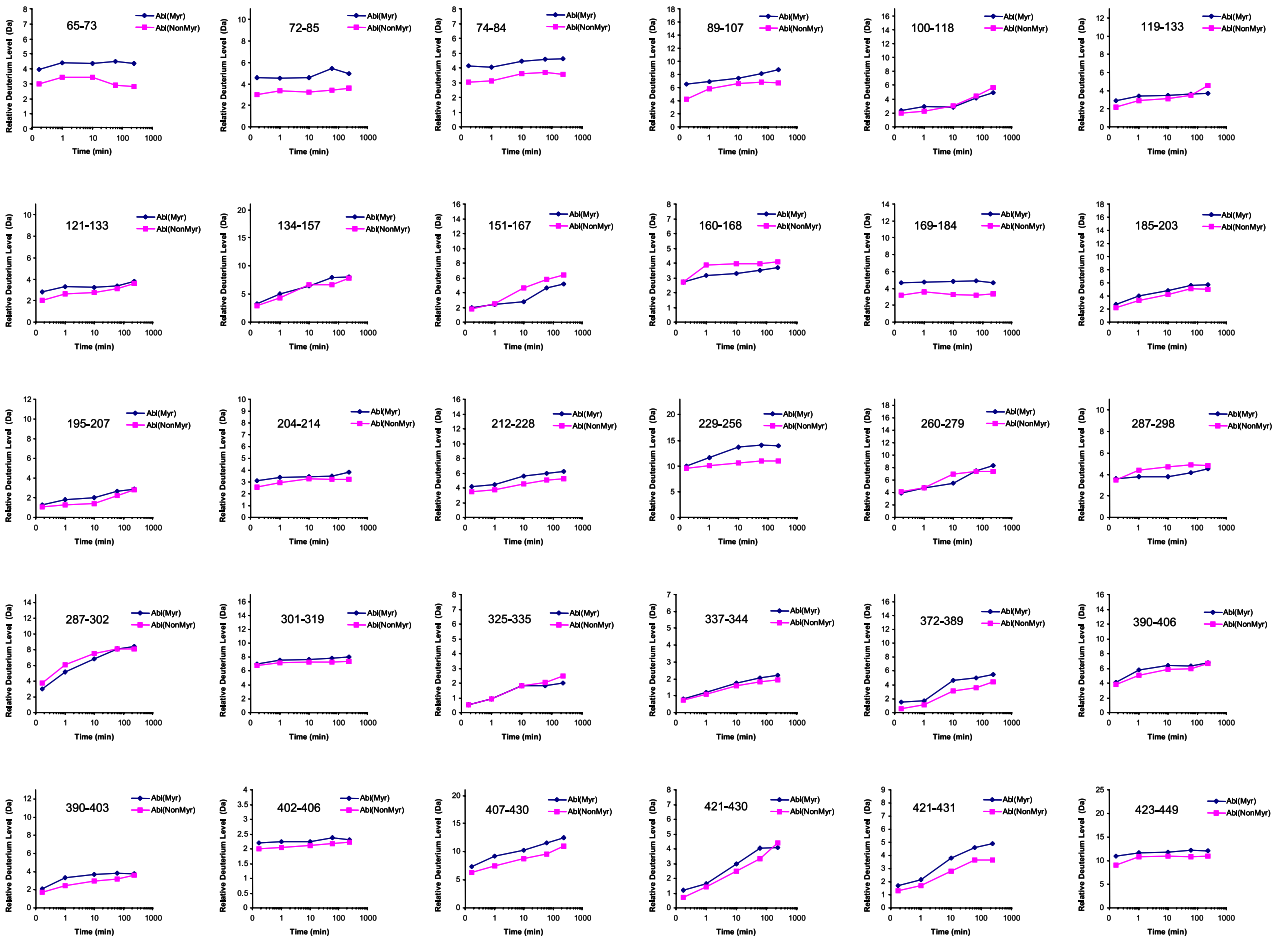

Fig. S7. Comparison of the relative deuterium incorporation curves for pepsin fragments from Abl(Myr) and Abl(NonMyr). The maximum of the *y* axis in each graph is the maximum amount of deuterium that could be incorporated. The data were obtained and processed as described in Fig. S4. Because these experiments were done as comparisons under identical experimental conditions, there was no correction made for back-exchange and all results are reported as relative deuterium level [Wales TE, Engen JR (2006) *Mass Spectrom Rev* 25:158–170]. Although the entire experiment was performed in duplicate, only 1 dataset is shown. The error of determining the deuterium levels was ±0.20 Da.

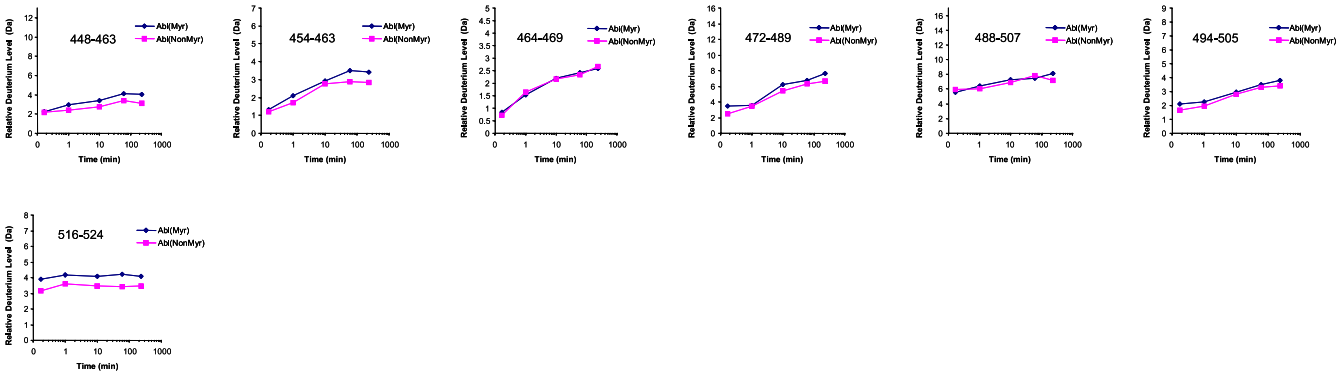

Fig. S7 (continued).

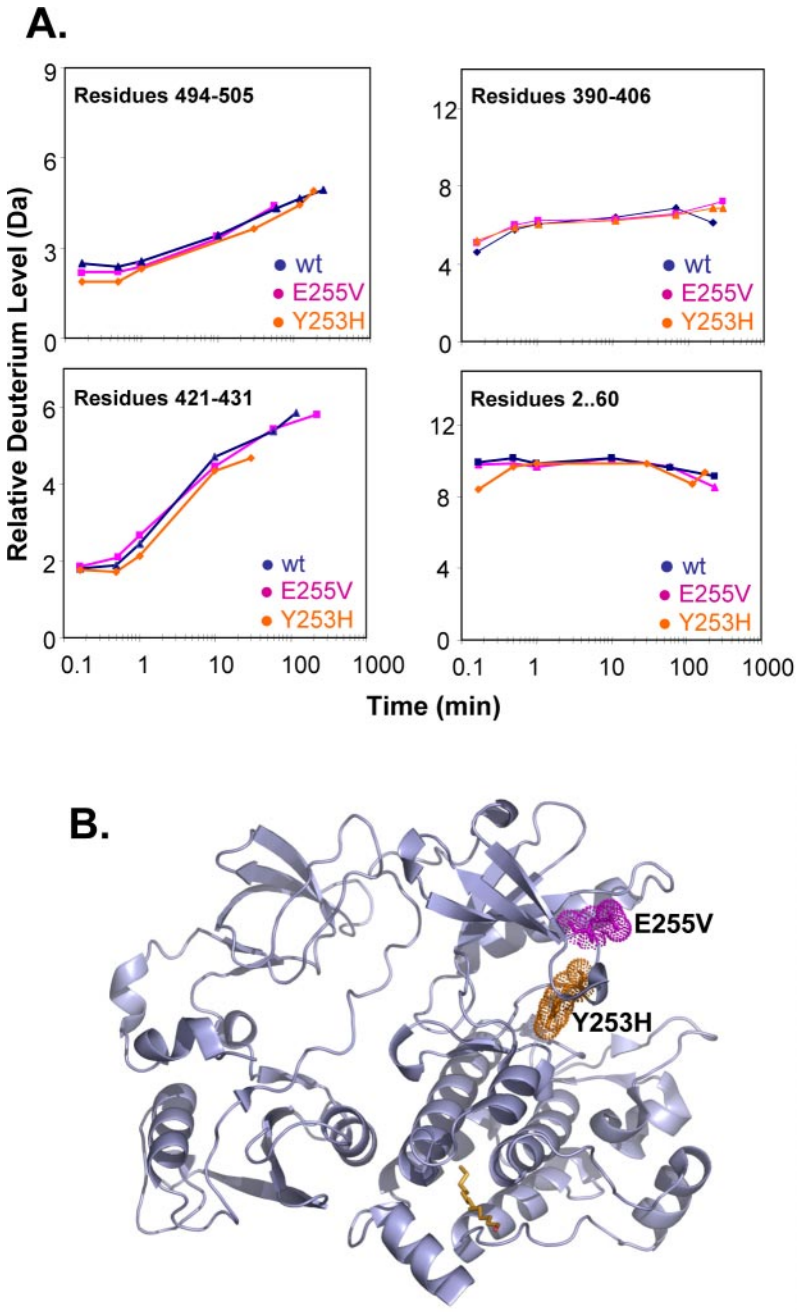

Fig. S8. Representative HX MS data for Abl(Myr), Abl(Myr)Y253H and Abl(Myr)E255V. The deuterium incorporation graphs of several regions are shown in *A*, and the location of the mutations is shown in *B* on the crystal structure of Abl [PDB entry 2FO0 (1)]. All of the data for all of the peptides of these 3 proteins looks similar to this: no visible differences were observed in any peptides. The data were obtained and processed as described in Fig. S4.

1. Nagar B, *et al.* (2006) Organization of the SH3-SH2 unit in active and inactive forms of the c-Abl tyrosine kinase. *Mol Cell* 21:787–798.

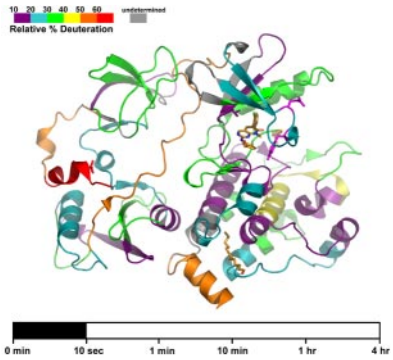

Movie S1. Data looking at the ''front'' (as traditionally defined) of the molecule shown in Fig. 1. The crystal structure used was PDB entry 2FO0 [Nagar B, *et al.* (2006) *Mol Cell* 21:787–798].

Movie S1 (MPG)

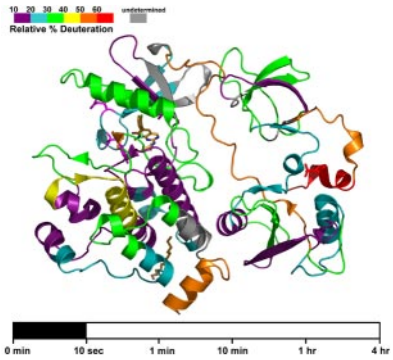

Movie S2. Data looking at the ''back'' of the molecule shown in Fig. 1. The crystal structure used was PDB entry 2FO0 [Nagar B, *et al.* (2006) *Mol Cell* 21:787–798].

Movie S2 (MPG)